

Fully Automatic 3D Glioma Extraction in Multi-contrast MRI

Pavel Dvorak^{1,2}(✉) and Karel Bartusek²

¹ Department of Telecommunications, Faculty of Electrical Engineering
and Communication, Brno University of Technology, Technicka 12,
612 00 Brno, Czech Republic

² Institute of Scientific Instruments of the ASCR, v.v.i., Kralovopolska 147,
612 64 Brno, Czech Republic
{pdvorak,bar}@isibrno.cz
<http://www.splab.cz>,
<http://www.isibrno.cz>

Abstract. This work deals with the fully automatic extraction of a glioma, the most common type of brain tumor, in multi-contrast 3D magnetic resonance volumes. The detection is based on the locating the area that breaks the left-right symmetry of the brain. The proposed method uses multi-contrast MRI, where FLAIR and T2-weighted volumes are employed. The algorithm was designed to extract the whole pathology as one region.

The created algorithm was tested on 80 volumes from publicly available BRATS databases containing multi-contrast 3D brain volumes afflicted by a brain tumor. These pathological structures had various sizes and shapes and were located in various parts of the brain. The extraction process was evaluated by Dice Coefficient(0.75). The proposed algorithm detected and extracted multifocal tumors as separated regions as well.

Keywords: Brain tumor · Image segmentation · MRI · Multi-resolution analysis · Symmetry analysis

1 Introduction

This work focuses on the first step in automatic brain tumor segmentation in Magnetic Resonance Images (MRI), the extraction of the whole pathological area. Nowadays, the brain tumor segmentation is a frequent research topic. Most methods are still semi-automatic, such as the Support Vector Machines (SVM) based method used in [14], and the proposed method could help to eliminate the need for human work, which could improve the efficiency of medical's work. The results from the proposed analysis could also help to detect the presence of this

This work was supported by SIX CZ.1.05/2.1.00/03.0072, GACR 102/12/1104 and COST CZ LD14091.

kind of pathological area in brain volume and automatically display the regions of interest to medicals.

Pattern recognition algorithms usually rely on the shape of the required objects. But the tumor shape varies in each case so other properties have to be used. The general properties of healthy brain are widely used as a prior-knowledge. One of them is the probability of tissues locations using probability brain atlas, which is used e.g. in [5] and [17]. Another widely used knowledge, which is used in this paper, is the sagittal symmetry of healthy brain. This approach is also used e.g. in [2], [16], [19] or [10]. Areas that break this symmetry are most likely parts of a tumor or any other type of pathological tissue.

Current methods usually also rely on T1-weighted contrast enhanced images [3]. This is the image that we are trying to avoid, since it requires contrast enhanced agent (usually gadolinium) to be injected into the patient blood, which breaks the non-invasivity of magnetic resonance.

The first part of the proposed method, the preliminary locating of this kind of pathological area, can be used as the first step in the automatic tumor segmentation process using whichever MR contrast or combination of more MR contrasts. More information about the suitability of particular MR contrasts and their comparison can be found in [7]. The subsequent extraction is performed using Otsu's thresholding technique [15].

2 Proposed Method

The main idea behind this work is to detect and locate anomalies in 3D brain volumes using symmetry analysis. The sagittal symmetry of healthy brain is a frequent knowledge used for pathological area detection.

The input of the whole process is a 3D magnetic resonance volume containing a tumor. The tumor detection process consists of several steps. The first step is the extraction of the brain followed by cutting the image. Since all images in testing BRATS database are skull stripped, this step was skipped during testing. However, there are several methods used for brain extraction from 3D volumes and could be used here, e.g. method described in [20].

From this new cut volume, the mid-sagittal plane should be detected, using e.g. [12] or [18], to correctly align the head. In the aligned volume, the asymmetric parts are located. Since the detection process is region-based rather than pixel-based, the method does not need a perfectly aligned volume.

2.1 Tumor Locating

At first, the input volume is divided into left and right halves. Assuming that the head has been aligned and the skull is approximately symmetric, the symmetry plane is parallel to y - z plane and divides the volume of detected brain into two parts of the same size. The algorithm goes through both halves symmetrically by a cubic block. The size of the block is computed from the size of the image. The step size is smaller than the block size to ensure the overlapping

of particular areas. These areas are compared with its opposite regions. Normalized histograms with the same range are computed for both cubic regions, left and right, and they are compared by Bhattacharya coefficient (BC) [1], which expresses the similarity of two sets. BC is computed as follows:

$$BC = \sum_{i=1}^N \sqrt{l(i) \cdot r(i)}, \quad (1)$$

where N denotes the number of bins in the histogram, l and r denote histograms of blocks in left and right half, respectively. The range of values of Bhattacharya coefficient is $[0, 1]$, where the smaller value means the bigger difference between histograms. For the next computation, the asymmetry is computed as $A = 1 - BC$.

This asymmetry is computed for all blocks. Since the regions overlap during the computation, the average asymmetry is computed for each pixel. The whole cycle is repeated three times but for different resolution of the volume. The resolution of each axis is iteratively reduced to the half of the previous value. This approach corresponds to the multi resolution image analysis described in [11]. The output of each cycle is an asymmetry map. The product of values corresponding to a particular pixel creates new multi-resolution asymmetry map. This computation is performed for each contrast volume separately. The example of the asymmetry map for multifocal tumor is shown in Figure 1.

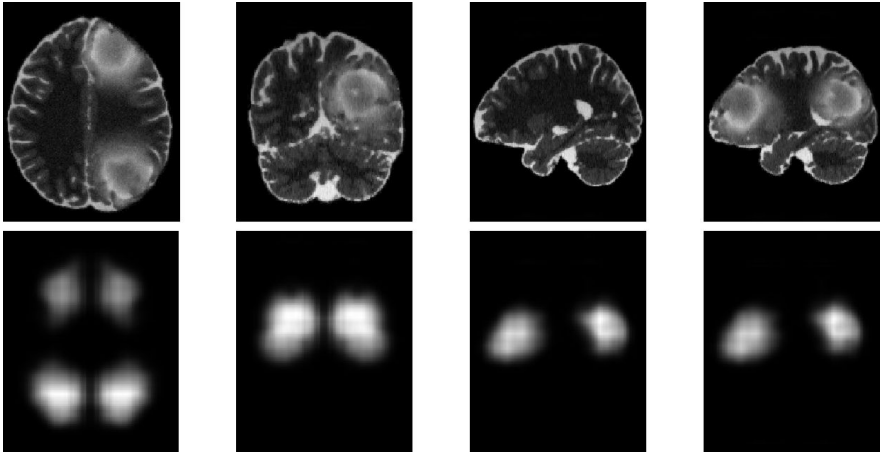


Fig. 1. Example of asymmetry map. The top row shows the T2 slices with the highest asymmetry. The bottom row shows the asymmetry maps of the T2-weighted volume of the corresponding slices.

For the pathology extraction purpose, the thresholding of the multi-resolution 3D asymmetry map is performed. The threshold is computed from the particular

asymmetry map as 30% of the maximal asymmetry. This was set experimentally and ensures that at least small region is extracted. The results of the both-sided mask that contains both the tumor on one side and the healthy tissue on the other side.

Since multifocal tumor can appear, the detection process is not limited to only one region. All regions created by thresholding are considered. As a result, multifocal tumors located in both halves asymmetrically can be correctly detected.

2.2 Tumor Extraction

For the extraction of the tumor area, the both-sided mask computed in previous step is used, which means the decision which parts contain tumor is not made here. The extraction process is based on the method proposed in [8]. Gliomas and edemas can be well separated from white and gray matter using T2-weighted volume, since they appear hyperintense in this MR contrast. The automatic thresholding is performed to extract these pathological areas.

The threshold is determined from the points inside the resulting mask of asymmetry detection using the technique proposed by Otsu in 1979 [15]. Since the pathological area could extend beyond the asymmetry area border, the thresholding process is applied to the whole volume. Morphological erosion and dilation are performed with the resulting mask of the thresholding process to smooth the region borders and separate regions connected by a thin area. Those regions situated mostly outside the asymmetry mask are eliminated.

Since Cerebrospinal fluid (CSF) appears hyperintense in T2-weighted images as well, the FLAIR volume is employed, because in this MR contrast, the CSF produces much weaker signal than the white matter and the tumor itself. Hence, the areas with the lower intensity than the median intensity (which is most likely the white matter intensity) in FLAIR volume are eliminated.

3 Testing

The method is not composed of a training and a testing phase as most current method are, therefore no division into training and testing data is performed and all the available volumes are considered to be testing.

3.1 Dataset

Brain tumor image data used in this work were obtained from the MICCAI 2012 Challenge on Multimodal Brain Tumor Segmentation organized by B. Menze, A. Jakab, S. Bauer, M. Reyes, M. Prastawa, and K. Van Leemput. The challenge database contains fully anonymized images from the following institutions: ETH Zurich, University of Bern, University of Debrecen, and University of Utah. (<http://www.imm.dtu.dk/projects/BRATS2012>)

The data contains real volumes of 20 high-grade and 10 low-grade glioma subjects and simulated volumes of 25 high-grade and 25 low-grade glioma subjects. All the simulated images are in BrainWeb space [4]. The information about the simulation method can be found in [17].

No attempt was made to put the individual patients in a common reference space and no modifications were needed for the testing dataset.

3.2 Evaluation Criteria

The extraction process is evaluated by the Dice Coefficient (DC) [6], which is computed according to the equation:

$$DC = \frac{2|A \cap B|}{|A| + |B|}, \quad (2)$$

where A and B denote the ground truth and the result masks of the extraction, respectively. The range of the DC values is $[0;1]$, where the 1 expresses the perfect segmentation.

4 Results

The results of extraction process are evaluated by Dice Coefficient are summarized in Table 1. Even though the maximum of the FLAIR and T2 asymmetry map was situated outside the ground truth in 3 of 80 cases, there was no intersection between ground truth and automatic extraction result only in 1 of them. In other words, even though the maximum was located outside the tumor, the extracted regions contained this pathological area.

Table 1. The Dice coefficient (DC) for pathological area extraction in particular sets

		Real Data		Simulated Data		Overall
		High Gr.	Low Gr.	High Gr.	Low Gr.	
DC	Mean	0.67 ± 0.22	0.78 ± 0.10	0.80 ± 0.10	0.72 ± 0.05	0.74 ± 0.14
	Median	0.75	0.78	0.82	0.71	0.75

It has to be stated that these results are for non-aligned volumes. The method would not work for highly rotated volumes, nevertheless since it is region-based rather than pixel-based, the perfect alignment is not necessary. According to [21], the $DC > 0.7$ indicates an excellent similarity. This statement was met for both high and low grade gliomas in both real and simulated data.

The examples of extraction results on the real data of the low grade glioma and the simulated data of the high grade multifocal glioma are shown in Figures 2 and 3, respectively. Slices with maximum asymmetry are shown in both figures. As can be seen in Figure 2, the precise vertical alignment of the head is not necessary.

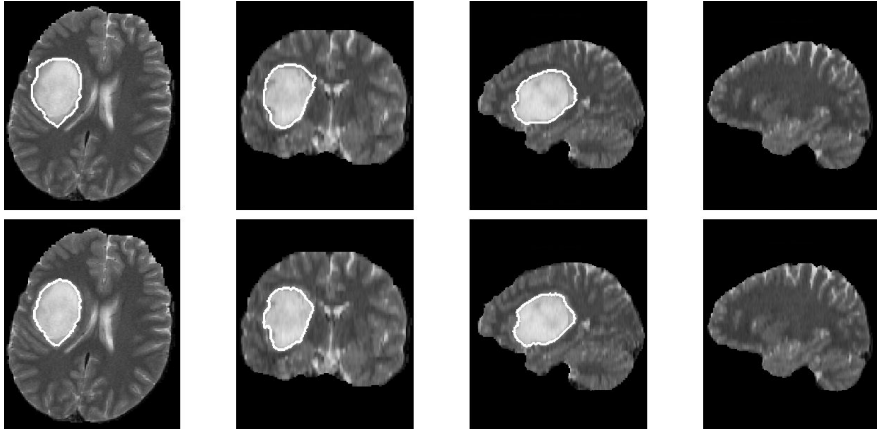


Fig. 2. Example of brain tumor extraction on volumes from real data of the low grade glioma with the $DC = 0.93$. The top and bottom rows show the ground truth and the automatic segmentation result, respectively.

Even though the proposed method was tested on publicly available BRATS 2012 database, the comparison with other methods is not straightforward. The MICCAI 2012 Challenge was focused on segmentation of tumor and edema separately. Hence, the described results in this paper cannot be compared to those described in the proceedings of MICCAI-BRATS 2012 [13]. On the other hand, our work is fully automated and does not require training phase as all methods proposed in the proceedings. Training phase requires normalized intensities in all involved images, which brings another inaccuracy into the segmentation process and cannot be always reached accurately. An alternative to intensity normalization is patient specific training dataset that requires manual selection of several points in foreground and background tissues.

5 Conclusion

The purpose of this work was to show an automatic brain tumor extraction technique for multi-contrast MRI. The proposed method reached promising results, but there are still areas for improving the extraction performance. The proposed algorithm automatically detected and extracted multifocal tumors as separated regions as well.

To improve the performance, the combination with the brain tissue probabilistic atlas or more sophisticated image segmentation algorithms such as Active Contour or Graph Cut will be considered. The attention of future work will also be paid on the automatic probabilistic determination of pathological area presence based on our previous method for 2D axial images [9] and separation of particular parts of pathology.

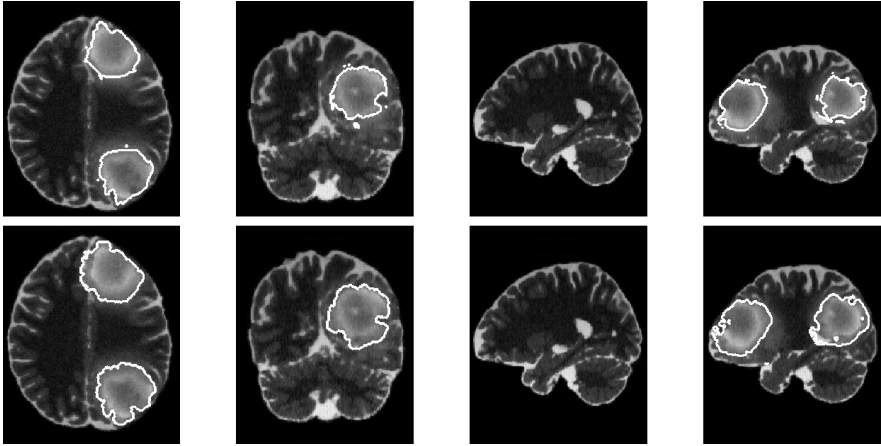


Fig. 3. Example of brain tumor detection on volumes from simulated data of high grade glioma with $DC = 0.80$. The top and bottom rows show the ground truth and the automatic segmentation result, respectively.

References

1. Bhattacharyya, A.: On a measure of divergence between two statistical populations defined by their probability distribution. *Bulletin of the Calcutta Mathematical Society* **35**, 99–110 (1943)
2. Cap, M., Gescheidtova, E., Marcon, P., Bartusek, K.: Automatic detection and segmentation of the tumor tissue. In: *Progress in Electromagnetics Research Symposium*, pp. 53–56 (2013)
3. Capelle, A.S., Colot, O., Fernandez-Maloinne, C.: Evidential segmentation scheme of multi-echo MR images for the detection of brain tumors using neighborhood information. *Information Fusion* **5**(3), 203–216 (2004). <http://www.sciencedirect.com/science/article/pii/S1566253503000848>
4. Cocosco, C.A., Kollokian, V., Kwan, R.K.S., Pike, G.B., Evans, A.C.: Brainweb: Online interface to a 3d mri simulated brain database. *NeuroImage* **5**, 425 (1997)
5. Cuadra, M.B., Pollo, C., Bardera, A., Cuisenaire, O., Villemure, J.G., Thiran, J.P.: Atlas-based segmentation of pathological mr brain images using a model of lesion growth. *IEEE Trans. Med. Imaging* **23**(1), 1301–1314 (2004)
6. Dice, L.R.: Measures of the amount of ecologic association between species. *Ecology* **26**(3), 297–302 (1945)
7. Dvorak, P., Bartusek, K.: Brain tumor locating in 3d mr volume using symmetry. In: *Proc. SPIE 9034, Medical Imaging 2014: Image Processing*, 903432 (2014)
8. Dvorak, P., Bartusek, K., Kropatsch, W.G.: Automated segmentation of brain tumor edema in flair mri using symmetry and thresholding. In: *Progress in Electromagnetics Research Symposium*, pp. 936–939 (2013)
9. Dvorak, P., Kropatsch, W.G., Bartusek, K.: Automatic brain tumor detection in t2- weighted magnetic resonance images. *Measurement Science Review* **13**(5), 223–230 (2013)

10. Khotanlou, H., Colliot, O., Bloch, I.: Automatic brain tumor segmentation using symmetry analysis and deformable models. In: Conf. on Advances in Pattern Recognition ICAPR, Kolkata, India (January 2007)
11. Kropatsch, W.G., Haxhimusa, Y., Ion, A.: Multiresolution image segmentations in graph pyramids. In: Kandel, A., Bunke, H., Last, M. (eds.) Applied Graph Theory in Computer Vision and Pattern Recognition. SCI, vol. 52, pp. 3–41. Springer, Heidelberg (2007)
12. Liu, Y., Collins, R.T., Rothfus, W.E.: Robust midsagittal plane extraction from normal and pathological 3-d neuroradiology image. *IEEE Transactions on Medical Imaging* **20**(3), 175–192 (2003)
13. Menze, B., Jakab, A., Bauer, S., Kalpathy-Cramer, J., Farahani, K., Kirby, J., Burren, Y., Porz, N., Slotboom, J., Wiest, R., Lanczi, L., Gerstner, E., Weber, M.A., Arbel, T., Avants, B., Ayache, N., Buendia, P., Collins, L., Cordier, N., Corso, J., Criminisi, A., Das, T., Delingette, H., Demiralp, C., Durst, C., Dojat, M., Doyle, S., Festa, J., Forbes, F., Geremia, E., Glocker, B., Golland, P., Guo, X., Hamamci, A., Iftekharuddin, K., Jena, R., John, N., Konukoglu, E., Lashkari, D., Antonio Mariz, J., Meier, R., Pereira, S., Precup, D., Price, S.J., Riklin-Raviv, T., Reza, S., Ryan, M., Schwartz, L., Shin, H.C., Shotton, J., Silva, C., Sousa, N., Subbanna, N., Szekely, G., Taylor, T., Thomas, O., Tustison, N., Unal, G., Vasseur, F., Wintermark, M., Hye Ye, D., Zhao, L., Zhao, B., Zikic, D., Prastawa, M., Reyes, M., Van Leemput, K.: The Multimodal Brain Tumor Image Segmentation Benchmark (BRATS), <http://hal.inria.fr/hal-00935640>
14. Mikulka, J., Gescheidtova, E.: An improved segmentation of brain tumor, edema and necrosis. In: Progress in Electromagnetics Research Symposium, pp. 25–28 (2013)
15. Otsu, N.: A Threshold Selection Method from Gray-level Histograms. *IEEE Transactions on Systems, Man and Cybernetics* **9**(1), 62–66 (1979). <http://dx.doi.org/10.1109/TSMC.1979.4310076>
16. Padoa, V., Binaghi, E., Balbi, S., De Benedictis, A., Monti, E., Minotto, R.: Glial brain tumor detection by using symmetry analysis. In: Proc. SPIE. vol. 8314, pp. 831445-1–831445-8 (2012), <http://dx.doi.org/10.1117/12.910172>
17. Prastawa, M., Bullitt, E., Moon, N., Van Leemput, K., Gerig, G.: Automatic brain tumor segmentation by subject specific modification of atlas priors. *Academic Radiology* **10**(12), 1341–1348 (2003)
18. Ruppert, G.C.S., Teverovskiy, L., Yu, C., Falcao, A.X., Liu, Y.: A new symmetry-based method for mid-sagittal plane extraction in neuroimages. In: International Symposium on Biomedical Imaging: From Macro to Nano (2011)
19. Saha, B.N., Ray, N., Greiner, R., Murtha, A., Zhang, H.: Quick detection of brain tumors and edemas: A bounding box method using symmetry. *Computerized Medical Imaging and Graphics* **36**(2), 95–107 (2012). <http://www.sciencedirect.com/science/article/pii/S0895611111000796>
20. Uher, V., Burget, R., Masek, J., Dutta, M.: 3d brain tissue selection and segmentation from mri. In: 2013 36th International Conference on Telecommunications and Signal Processing (TSP), pp. 839–842 (2013)
21. Zijdenbos, A., Dawant, B.: Brain segmentation and white matter lesion detection in mr images. *Critical Reviews in Biomedical Engineering* **22**, 401–465 (1994)